Biochemical properties and *in planta* effects of NopM, a rhizobial E3 ubiquitin ligase

Received for publication, June 15, 2018, and in revised form, July 25, 2018 Published, Papers in Press, August 17, 2018, DOI 10.1074/jbc.RA118.004444

Chang-Chao Xu[‡], Di Zhang[‡], Dagmar R. Hann[§], Zhi-Ping Xie[‡¶1], and Christian Staehelin[‡¶2]

From the [‡]State Key Laboratory of Biocontrol and Guangdong Key Laboratory of Plant Resources, School of Life Sciences, Sun Yat-sen University, East Campus, Guangzhou 510006, China, the [§]Institute of Genetics, Ludwig-Maximilians-Universität München, D-82152 Martinsried, Germany, and the [¶]Shenzhen Research and Development Center of State Key Laboratory of Biocontrol, School of Life Sciences, Sun Yat-sen University, Baoan, Shenzhen 518057, China

Edited by George N. DeMartino

Nodulation outer protein M (NopM) is an IpaH family type three (T3) effector secreted by the nitrogen-fixing nodule bacterium *Sinorhizobium* sp. strain NGR234. Previous work indicated that NopM is an E3 ubiquitin ligase required for an optimal symbiosis between NGR234 and the host legume *Lablab purpureus*. Here, we continued to analyze the function of NopM. Recombinant NopM was biochemically characterized using an *in vitro* ubiquitination system with *Arabidopsis thaliana* proteins. In this assay, NopM forms unanchored polyubiquitin chains and possesses auto-ubiquitination activity. In a NopM variant lacking any lysine residues, auto-ubiquitination was not completely abolished, indicating non-canonical auto-ubiquitination of the protein. In addition, we could show intermolecular ubiquitin transfer from NopM to C338A (enzymatically inactive NopM form) *in vitro*. Bimolecular fluorescence complementation analysis provided clues about NopM–NopM interactions at plasma membranes *in planta*. NopM, but not C338A, expressed in tobacco cells induced cell death, suggesting that E3 ubiquitin ligase activity of NopM induced effector-triggered immunity responses. Likewise, expression of NopM in *Lotus japonicus* caused reduced nodule formation, whereas expression of C338A showed no obvious effects on symbiosis. Further experiments indicated that serine residue 26 of NopM is phosphorylated *in planta* and that NopM can be phosphorylated *in vitro* by salicylic acid–induced protein kinase (NtSIPK), a mitogen-activated protein kinase (MAPK) of tobacco. Hence, NopM is a phosphorylated T3 effector that can interact with itself, with ubiquitin, and with MAPKs.

Type III protein secretion systems (T3SSs)[3] are powerful weapons of many pathogenic Gram-negative bacteria. By using a needle-like pilus, the T3SS apparatus has the capacity to translocate effector proteins into eukaryotic host cells (1). Secretion and translocation of type III (T3) effectors require a serine-rich N terminus that contains intrinsic disorder regions (2). Within host cells, T3 effectors manipulate cell metabolism in different ways to increase bacterial virulence (1, 3). However, when directly or indirectly recognized by plant cells, specific T3 effectors may function as avirulence proteins that elicit programmed cell death (also called hypersensitive response). Consequently, bacterial growth is impaired in these plants (effector-triggered immunity (ETI)) (4). Some symbiotic bacteria, such as rhizobia, also possess T3SSs (5, 6). These bacteria infect legume roots and differentiate into nitrogen-fixing bacteroids in formed root nodules. Fixed nitrogen is then transported to the host plant, which feeds the bacteria with assimilates and nutrients (7). Depending on the host legume, rhizobial effectors may play positive or negative roles in symbiosis. Accordingly, mutant strains lacking the T3SS apparatus or effector genes can have promoting or inhibiting effects on nodule formation and nitrogen fixation (5, 6). However, compared with T3 effectors of pathogenic bacteria, knowledge on rhizobial T3 effectors is limited. Similar to pathogenic effectors, at least some rhizobial T3 effectors interfere with host defense signaling, and successful symbiosis may depend on the rhizobial ability to suppress plant defense reactions (8–12). In addition, rhizobial T3 effectors eventually activate nodulation signaling of host plants (13). Negative effects of some rhizobial T3 effectors on nodulation are likely due to direct or indirect recognition by host resistance proteins (14) and subsequent induction of ETI-like plant defense responses (15).

The T3 effector NopM (nodulation outer protein M) was first identified in *Sinorhizobium* (*Ensifer*) *fredii* strain HH103

This work was supported by the National Natural Science Foundation of China Grant 31470197; by the Department of Science and Technology of Guangdong Province, China, Grants 2013B051000043 and 2017B030311005; by the Science Foundation of the State Key Laboratory of Biocontrol Grants SKLBC32-2017-A09 and SKLBC32-2018-A10; and by the Guangdong Key Laboratory of Plant Resources Grant 2014B030301026. The authors declare that they have no conflicts of interest with the contents of this article.

This article contains Figs. S1–S5 and Tables S1–S2.

[1] To whom correspondence may be addressed. E-mail: xiezping@mail.sysu.edu.cn.

[2] To whom correspondence may be addressed. E-mail: cst@mail.sysu.edu.cn.

[3] The abbreviations used are: T3SS, type III protein secretion system; APase, alkaline phosphatase; E1, enzyme 1 of the ubiquitination system (ubiquitin-activating enzyme); E2, enzyme 2 of the ubiquitination system (ubiquitin-conjugating enzyme); E3, enzyme 3 of the ubiquitination system (ubiquitin ligase); ETI, effector-triggered immunity; GST, glutathione *S*-transferase, LRR, leucine-rich repeats; MAPK, mitogen-activated protein kinase; NEL domain, novel E3 ubiquitin ligase domain; Nop, nodulation outer protein; RFP, red fluorescent protein; ROS, reactive oxygen species; YFP, yellow fluorescent protein; T3, type III; Ub, ubiquitin; BiFC, bimolecular fluorescence complementation; CaMV, cauliflower mosaic virus.

(16). Mutant analysis showed that NopM of *Sinorhizobium* sp. strain NGR234 promotes symbiosis in the interaction with the host plant *Lablab purpureus* (11, 17). The use of a *Xanthomonas/Capsicum* translocation system indicated that NopM is translocated into plant cells (18). When expressed in *Nicotiana benthamiana* plants treated with the flagellin peptide flg22 (an elicitor of plant defense reactions), NopM inhibited production of reactive oxygen species (ROS) but stimulated induction of defense genes (11). NopM is a member of the IpaH (Invasion-plasmid antigen H) effector family that is present in various human pathogens such as *Shigella flexneri* (19–22) and *Salmonella enterica* (23, 24). Recently, related effectors (RipAW and RipAR) have also been identified in the plant pathogen *Ralstonia solanacearum* (25). NopM, like other IpaH family effectors, consists of a variable N-terminal domain containing leucine-rich repeats (LRR domain) and a conserved C-terminal novel E3 ubiquitin ligase (NEL) domain. NopM possesses E3 ubiquitin ligase activity in an *in vitro* system with commercially available mammalian proteins (11).

Ubiquitination in eukaryotic cells can affect proteins in many ways. For example, it can function as a signal for their degradation via the 26S proteasome, alter their subcellular localization, influence their activity, and affect protein–protein interactions. Three key enzymes are involved in the ubiquitination reaction. First, a ubiquitin-activating enzyme (E1) forms a thioester bond between the E1 cysteine sulfhydryl group and the C-terminal carboxyl group (di-glycine motif, GG) of ubiquitin in an ATP-consuming step. Then, the activated ubiquitin is transferred to a ubiquitin-conjugating enzyme (E2). Finally, a ubiquitin ligase (E3) transfers the activated ubiquitin from a ubiquitin-loaded E2 to the ϵ-amino group of a given lysine residue in the protein substrate, thus forming a glycine–lysine isopeptide bond (26). The bacterial IpaH family of E3 ubiquitin ligases possesses a reaction mechanism that is similar to eukaryotic HECT-type E3 proteins. The ubiquitin-accepting cysteine residue and the catalytic acid (aspartic acid) are located in a single conserved C*X*D (*X* means any amino acid) motif that is crucial for enzyme activity (Fig. S1) (21, 27). Accordingly, the enzymatically inactive NopM variant C338A (substitution of cysteine 338 to alanine; Fig. S2) lacks E3 ubiquitin ligase activity and consequently did not show a positive effect on nodulation of *L. purpureus* (11). IpaH family effectors can form free (unanchored) polyubiquitin chains that contain glycine–lysine isopeptide bonds between two ubiquitin molecules. Detailed studies on the IpaH9.8 effector of *S. flexneri* showed that Lys-48 is the predominant lysine residue for linkage formation (21, 28). Lys-48 –linked polyubiquitin chains are the principal targeting signal for proteasomal degradation. Accordingly, ubiquitinated substrates of IpaH9.8, such as human guanylate-binding proteins (29, 30), are rapidly degraded. As ubiquitin possesses seven lysine residues, formation of polyubiquitin chains with different linkages is possible, and this can lead to branched polyubiquitin (31, 32). IpaH family effectors may possess auto-ubiquitination activity. Analysis of *in vitro* reactions with IpaH9.8 indicated that Lys-48-linked polyubiquitin chains were not only free but also anchored to IpaH9.8 itself (28).

In this study, we used an *in vitro* ubiquitination system with *Arabidopsis thaliana* proteins to biochemically characterize NopM of *Sinorhizobium* sp. NGR234. We found that NopM preferentially catalyzes unanchored Lys-48 – dependent polyubiquitination reactions but also possesses auto-ubiquitination activity. Surprisingly, noncanonical auto-ubiquitination activity was observed for a NopM variant that does not possess any lysine residue. Furthermore, we found evidence for intermolecular transfer of ubiquitin from NopM to C338A (enzymatically inactive NopM form). We also provide clues to NopM–NopM interactions at plasma membranes. To study effector function *in vivo*, we expressed NopM and C338A in plants. Cell death in tobacco and impaired nodulation of *Lotus japonicus* were observed for NopM but not for C338A, suggesting that E3 ligase activity is responsible for these effects. Furthermore, we found that a serine residue of NopM is phosphorylated *in vivo* and *in vitro* and that NopM is a mitogen-activated protein kinase (MAPK) substrate.

Results

Ubiquitination reactions with NopM and variants

To study the enzyme activity of NopM and variants *in vitro*, we cloned *A. thaliana* genes encoding an E1 and an E2 (E1, AtUBA2; E2, AtUBC10) enzyme. Furthermore, we cloned 228 bp of the *A. thaliana* polyubiquitin precursor gene *UBQ14* (At4g02890) encoding ubiquitin. All genes were expressed in *Escherichia coli* with a polyhistidine tag (His tag), and proteins were purified by nickel affinity chromatography. Incubation of purified E1, E2, and ubiquitin in combination with NopM resulted in formation of polyubiquitin chains that can be detected with an anti-ubiquitin antibody. Bands with a molecular mass lower than NopM (≈60.5 kDa) indicated the presence of free polyubiquitin chains in the reaction mixture (multiples of His-tagged ubiquitin). Western blot analysis with the anti-NopM antibodies showed additional bands above NopM, indicating auto-ubiquitination of NopM. Formation of polyubiquitin chains and auto-ubiquitination activity were increased when the NEL protein (truncated NopM containing only the C-terminal NEL domain) was used in the assay (Fig. 1*A*).

Ubiquitin possesses seven lysine residues, and different lysine– glycine linkages may exist in polyubiquitin chains. To characterize the linkage preference of NopM, we performed ubiquitination reactions with ubiquitin variants in which one of the seven lysine residues was substituted by arginine. Formation of polyubiquitin chains with the K48R ubiquitin variant was lower than with nonmodified ubiquitin or the other tested ubiquitin forms, indicating that NopM preferentially produces Lys-48 – dependent polyubiquitin chains. Reduced polyubiquitination with the K48R variant compared with ubiquitin was also observed for the NEL protein variant (Fig. 1*B*). Remarkably, auto-ubiquitination of NopM with the K48R variant was stronger than with ubiquitin under these test conditions. Similar results were also obtained for the NEL protein (Fig. 1*C*). These findings suggest that NopM possesses several ubiquitination sites that were mono-ubiquitinated with K48R. Furthermore, auto-ubiquitination of NopM seems to become stronger when ubiquitin is not used up for formation of polyubiquitin chains. An experiment with human USP5 supported this hypothesis. This enzyme preferentially depolymerizes unanchored polyu-

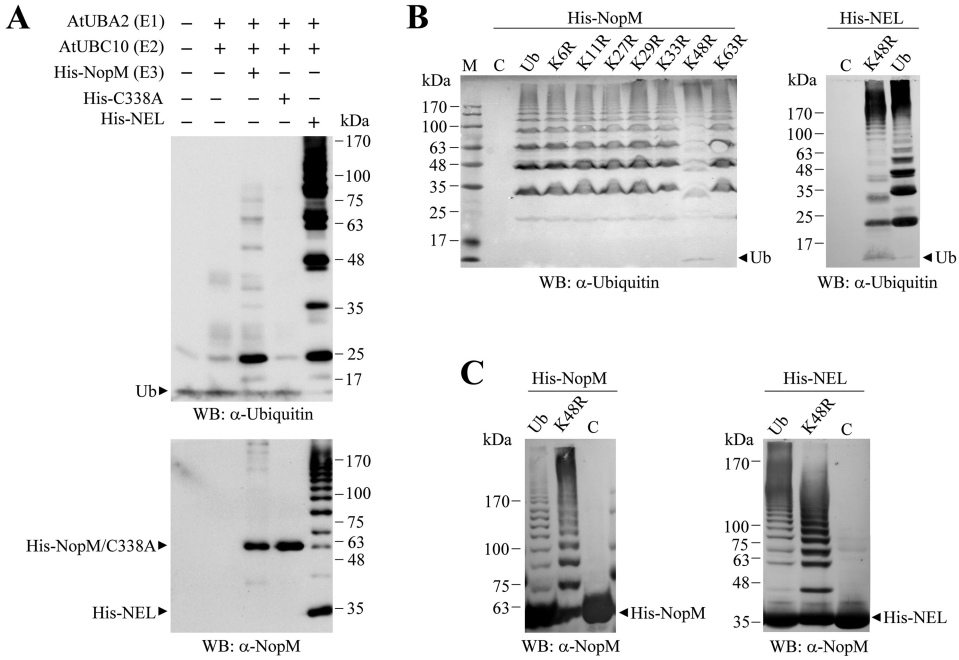

Figure 1. Ubiquitination reactions catalyzed by NopM and variants. *A,* Western blot (*WB*) analysis of ubiquitination reactions with NopM and the variants C338A (no activity) and NEL (increased activity). Recombinant E1, E2, and Ub proteins of *A. thaliana* were used for the reactions. Western blottings were developed with anti-ubiquitin (*top*) or anti-NopM (*bottom*) antibodies. *B* and *C,* ubiquitination reactions catalyzed by NopM or NEL with ubiquitin or indicated ubiquitin variants with lysine to arginine substitutions. Control reactions without ubiquitin are also shown (*lanes C*). Western blot analysis was performed with anti-ubiquitin (*B*) or anti-NopM (*C*) antibodies. *Lane M*, molecular weight markers.

biquitin chains and therefore increases the concentration of monomeric ubiquitin in the reaction mixture (28, 33). Accordingly, auto-ubiquitination of NopM in the presence of recombinant USP5 was considerably increased, and Western blotting signals representing ubiquitinated NopM were comparable with those obtained from reactions with the K48R ubiquitin variant (Fig. S3).

Auto-ubiquitination of K3xR, a NopM variant without lysine residues

Sequence analysis of NopM indicated that NopM contains three lysine residues in the C-terminal NEL domain (Lys-502, Lys-531, and Lys-537). We therefore expected that substitution of these lysine residues to arginine abolishes auto-ubiquitination of NopM. However, Western blot analysis with the anti-NopM antibody indicated auto-ubiquitination of His–K3xR, a His-tagged NopM variant in which all three lysine residues were substituted by arginine. In contrast, auto-ubiquitination was not observed when ATP was omitted in the reaction (Fig. 2*A*). As N-terminal ubiquitination has been reported for certain proteins (34, 35), we analyzed whether removal of the N-terminal His tag by thrombin has an effect on auto-ubiquitinated His–K3xR. Incubation of the sample with thrombin resulted in an expected band shift on the Western blot, indicating formation of ubiquitinated K3xR forms without the His tag (Fig. 2*B*). Auto-ubiquitination of His–K3xR was also detected when GST–Ub (ubiquitin with an N-terminal GSH *S*-transferase (GST) tag) was used in the auto-ubiquitination assay. In contrast, a corresponding ladder of ubiquitinated His–K3xR forms was not observed in a parallel reaction with His–UbΔGG (His-tagged ubiquitin without C-terminal di-glycine residues) (Fig. 2*C*).

Moreover, we found that an enzymatically inactive K3xR variant, His–K3xR–C338A (His-tagged K3xR with cysteine residue 338 substituted by alanine), could function as acceptor for intermolecular transfer of ubiquitin. A band corresponding to mono-ubiquitinated His–K3xR–C338A was detected on Western blots when GST–NopM was used as ubiquitin ligase (Fig. 2*D*).

NopM–NopM interactions and subcellular localization of NopM

To study interactions between NopM molecules in more detail, we used enzymatically active (NopM and NEL) and inactive (C338A or C338S) protein forms with different tags for *in vitro* ubiquitination reactions. Western blot analysis showed that the Flag-tagged C338A or C338S proteins were ubiquitinated by GST-fused NopM, indicating an intermolecular transfer of ubiquitin (Fig. 3*A*). Flag-tagged C338A was also ubiquitinated by His-tagged NopM. However, the His-tagged NEL protein was unable to ubiquitinate Flag-tagged C338A. Likewise, neither His-tagged NEL nor His-tagged NopM could ubiquitinate Flag-tagged NEL(C338A), an enzymatically inactive NEL form with a cysteine-to-alanine substitution (Fig. S4). Hence, full-length sequences of NopM (donor) and C338A (acceptor) were required for intermolecular transfer of ubiquitin from NopM to C338A.

To test physical protein interactions *in planta*, we used a bimolecular fluorescence complementation (BiFC) method that is based on enhanced yellow fluorescent protein (YFP). Considering that the interaction between NopM molecules may depend on the LRR domain of NopM, we fused nYFP (N-terminal part of YFP) and cYFP (C-terminal part of YFP) to the C terminus of NopM to produce NopM–nYFP and NopM–

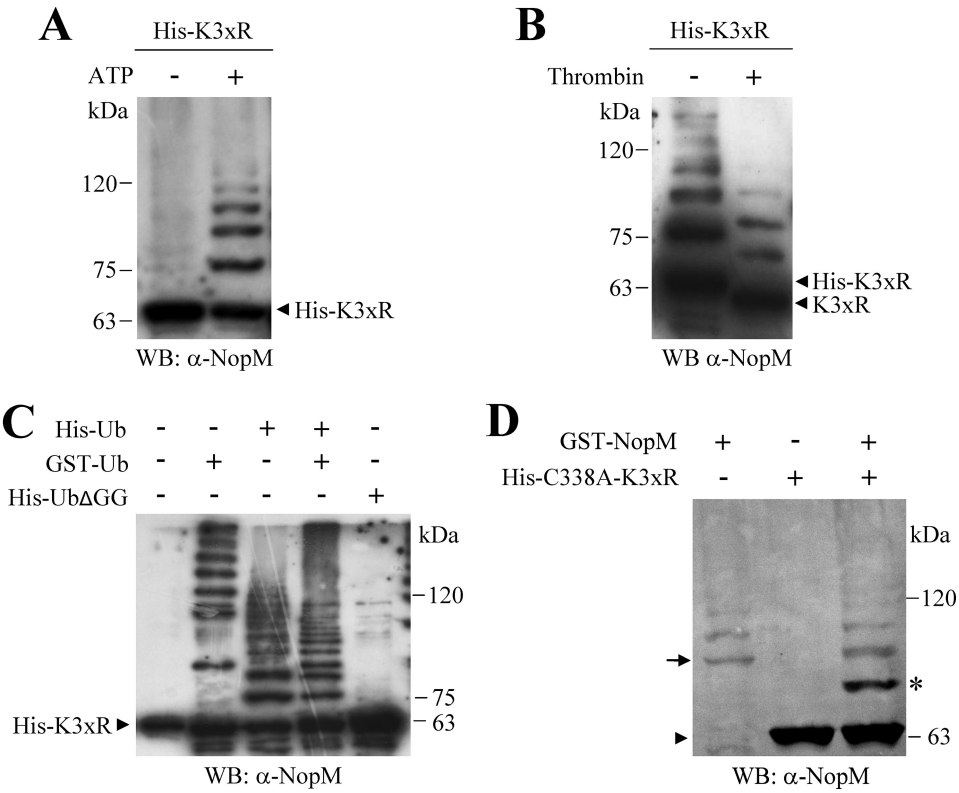

Figure 2. K3xR variant shows auto-ubiquitination activity. *A–C*, His-tagged K3xR protein (NopM with K502R, K531R, and K537R substitutions) was used for ubiquitination reactions (2 h), and auto-ubiquitination was detected with the anti-NopM antibody. Nonubiquitinated K3xR is marked by *arrowheads*. *A,* reactions (2 h) were performed with (+) or without (−) ATP. *B,* incubation of reaction products with and without thrombin (removal of the N-terminal His tag). *C,* reactions with GST-tagged ubiquitin, His-tagged ubiquitin, with a mixture (Ub mix; GST- and His-tagged ubiquitin, 1:1), or with UbΔGG (Ub without C-terminal di-glycine residues). *D,* analysis of intermolecular transfer of His-tagged ubiquitin from GST–NopM to His-tagged K3xR-C338A (NopM with C338A, K502R, K531R, and K537R substitutions). Nonubiquitinated His–K3xR–C338A is marked by an *arrowhead*, mono-ubiquitinated His–K3xR–C338A by an *asterisk*, and GST–NopM by an *arrow*. *WB*, Western blot.

cYFP fusion proteins. Plasmids expressing NopM–cYFP and nYFP or NopM–nYFP and cYFP served as negative controls. NopM constructs were delivered into onion cells by particle bombardment. Distinct yellow fluorescence signals at plasma membranes were observed for the combination NopM–nYFP with NopM–cYFP. Such signals were not detected for the controls (Fig. 3*B*). These results suggest dimerization of NopM at plasma membranes.

Furthermore, subcellular localization studies were performed for full-length NopM proteins that contained either a C-terminal green fluorescent protein (GFP) tag or an N-terminal red fluorescent protein (RFP) tag. Onion cells expressing these fusion proteins showed fluorescence in the whole cell. However, fluorescence signals associated with the nucleus were not as strong as those of the fluorescent proteins alone (Fig. 3, *C* and *D*). A similar fluorescence pattern was obtained for *A. thaliana* protoplasts expressing NopM–GFP or C338A–GFP fusion proteins (Fig. S5).

NopM induces cell death in tobacco

In the course of the performed subcellular localization studies, we noticed that NopM caused cell death when expressed in tobacco plants. NopM and variants were transiently expressed in leaves infiltrated with *Agrobacterium tumefaciens* carrying a given binary vector (containing a CaMV 35S promoter, the *nopM*-coding sequence, and an additional GFP expression cassette). A similar cell death response, albeit less pronounced, was also observed when the NEL protein was expressed in tobacco. In contrast, enzymatically inactive NopM variants (C338A and C338S) did not cause cell death, suggesting that ubiquitination of an unknown NopM substrate (or auto-ubiquitinated NopM) was required for cell death induction (Fig. 4*A*).

Western blot analysis with anti-NopM antibodies and anti-GFP antibodies confirmed that NopM and variants were expressed in transformed tobacco cells. As compared with the C338A variant, Western blot signals of NopM (≈61 kDa) and the NEL form (≈35 kDa) were fainter, indicating low protein levels in tissue that becomes necrotic. In addition to the NopM band, an upper band (≈70 kDa) was occasionally detected that likely corresponded to a mono-ubiquitinated NopM form. A similar upper band was always detected for the C338S variant (Fig. 4*B*). The upper band disappeared when the tobacco proteins containing C338S were incubated under mild alkaline conditions (Fig. 4*C*), providing clues for formation of an oxyester bond between serine and the C-terminal glycine of ubiquitin (36).

Expression of NopM in L. japonicus impairs nodule formation

To study whether NopM activity in *L. japonicus* influences symbiosis, we performed nodulation tests with *L. japonicus* expressing either NopM or the enzymatically inactive variant C338A. Co-expressed RFP was used to remove nontransgenic

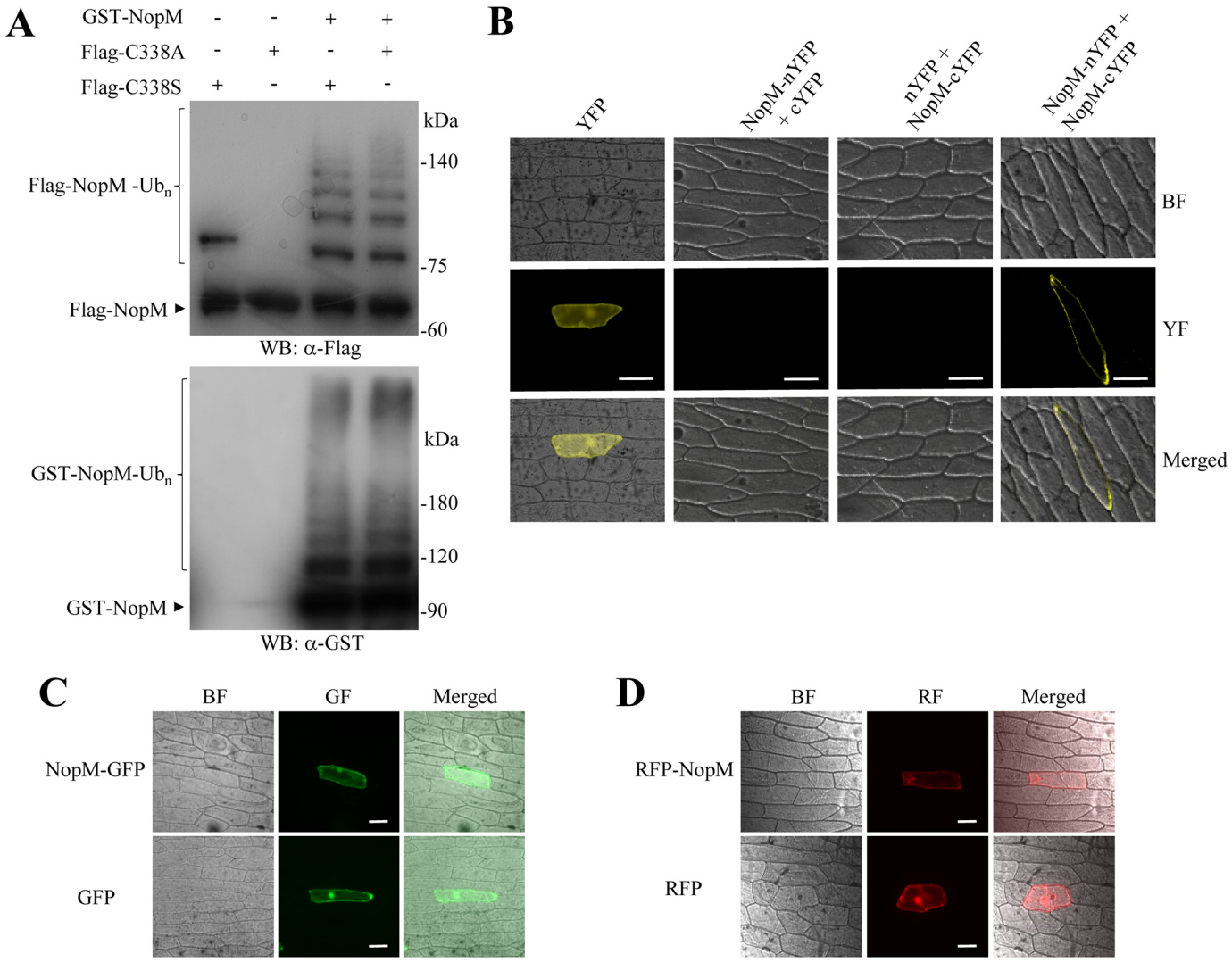

Figure 3. Analysis of NopM–NopM interactions and subcellular localization of NopM fused to fluorescent proteins. *A,* analysis of intermolecular transfer of ubiquitin *in vitro*. The Flag-tagged NopM variants C338A (enzymatically inactive) and C338S (forming a mono-ubiquitinated conjugate) were ubiquitinated by GST–NopM. Western blot (*WB*) were probed with anti-Flag or anti-GST antibodies. *B,* BiFC analysis of NopM–NopM interactions *in vivo*. Onion cells expressing indicated protein combinations were microscopically analyzed for yellow fluorescence (*YF*) emission and under bright field (*BF*) illumination. Co-expression of NopM–nYFP with NopM– cYFP resulted in formation of a BiFC complex at plasma membranes. *Bars*, 100 μm. *C* and *D,* subcellular localization of full-length NopM fusion proteins. Fluorescent NopM proteins with C-terminal GFP tag (*C*) or with N-terminal RFP tag (*D*) were expressed in onion cells. GFP and RFP alone were expressed for comparison. Emission of green fluorescence (*GF*), red fluorescence (*RF*), and bright field conditions were used for microscopic examination. *Bars*, 100 μm.

roots prior to rhizobial inoculation. RFP-expressing plants transformed with the vector alone served as a control. Western blot analysis with anti-NopM antibodies showed that both proteins were expressed, albeit signals for C338A were stronger than those for NopM (Fig. 5*A*). Plants were inoculated with the symbiont *Mesorhizobium loti* MAFF303099 (GFP) that constitutively expresses GFP. Microscopic fluorescence detection revealed that formed RFP-expressing nodules contained GFP-expressing bacteria (Fig. 5*B*). NopM-expressing roots formed smaller and fewer nodules than control plants transformed with the empty vector. Accordingly, the biomass of nodules per plant was significantly reduced, indicating that NopM expression impaired nodulation. Most nodules on NopM-expressing roots were pink (expression of leghemoglobin), suggesting that nitrogen fixation of bacteroids was not impaired. In contrast, C338A expression in *L. japonicus* did not show an obvious effect on nodulation, indicating that NopM activity was required to cause a negative effect on symbiosis (Fig. 5*C*).

NopM is a phosphorylated effector

NopM was found to interfere with mating pheromone signaling in yeast, suggesting that NopM interacts with components of a MAPK pathway (11). Moreover, protein analysis by gel electrophoresis indicated that the apparent molecular weight of NopM expressed in tobacco was slightly higher than the theoretical value predicted by computation. We therefore suggested that NopM expressed in plant cells is post-translationally modified by protein kinases. To test this hypothesis, aliquots of soluble protein extracts of NopM-expressing tobacco leaves were treated with calf intestine alkaline phosphatase (APase) and then analyzed on Western blots with anti-

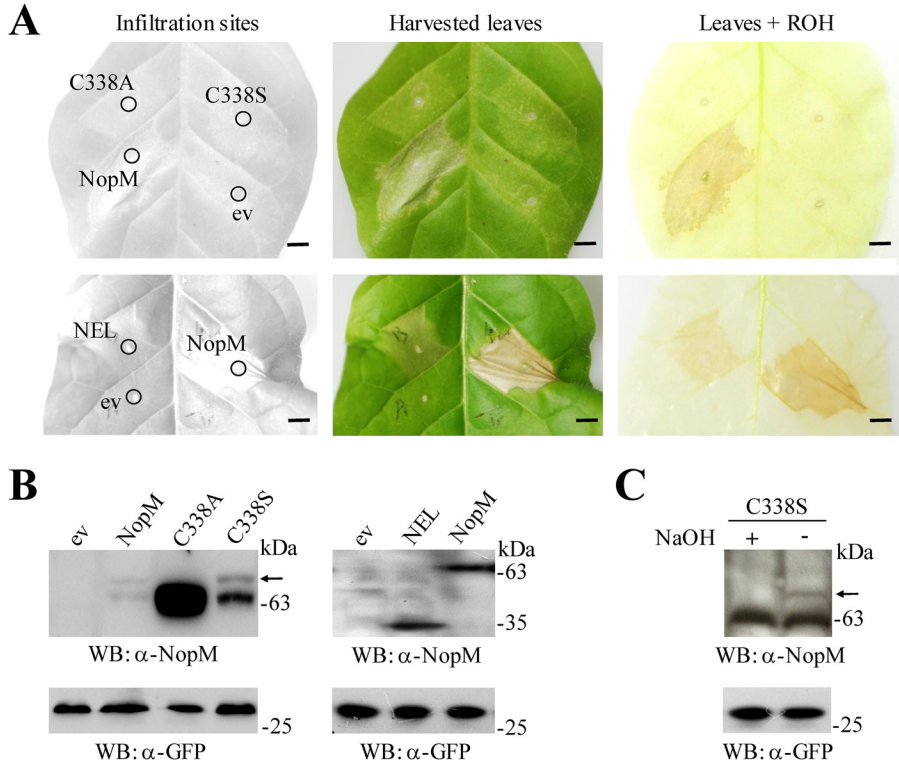

Figure 4. Expression of NopM and variants in tobacco. *A,* photographs of tobacco leaves expressing NopM, NEL, C338A, and C338S, respectively. *A. tumefaciens* carrying the empty vector (*ev*) was used as a negative control. Photographs were taken 3 days after infiltration of the bacterial suspensions. Harvested leaves were decolorized by boiling in ethanol (*ROH*) to visualize necrotic tissue. *Bars,* 0.5 cm. *B,* Western blot (*WB*) analysis of expressed proteins. Crude proteins from transformed tobacco leaves were isolated 2 days after infiltration with agrobacteria. Western blots were performed with 5 μl of the prepared extract and anti-NopM or anti-GFP antibodies. The *upper bands* (above NopM and C338S; marked by an *arrow*) likely represent mono-ubiquitinated forms. *C,* treatment of extracted C338S with 100 mM NaOH (final concentration) resulted in disappearance of the upper band, suggesting ubiquitination on the serine residue by formation of an oxyester bond.

NopM antibodies. NopM samples treated with APase migrated faster than nontreated controls. The APase treatment also caused band shifts for protein extracts of tobacco plants producing the C338A or C338S variants (Fig. 6*A*). These findings indicated that NopM was phosphorylated in tobacco plants.

The serine residue 26 (Ser-26) of NopM is followed by a proline. Such SP sites are typical motifs in MAPK substrates (12, 37). Moreover, bioinformatic analysis with NetPhos 3.1 predicted that serine 26 is a possible phosphorylation site in NopM. We therefore expressed S26A in tobacco (NopM variant in which Ser-26 is replaced by alanine). Protein extracts from transformed tissue were treated with and without APase as before. Different from NopM, no band shift could be detected for S26A on a Western blot (Fig. 6*A*), indicating that Ser-26 is indeed a phosphorylation site of NopM. Protein levels of S26A in transformed tobacco leaves were higher than those of NopM, whereas bands of co-expressed GFP were similar (Fig. 6*B*). Like NopM, expression of S26A induced cell death of the transformed tobacco tissue (Fig. 6*C*).

Furthermore, we carried out an *in vitro* phosphorylation assay with recombinant proteins expressed in *E. coli* (His-tagged NopM; GST-tagged protein kinases). NtSIPK, a MAPK of tobacco known to be activated by the upstream MAPK kinase NtMEK2^{DD}, was used as a representative kinase (38, 39). Reaction mixtures were subjected to Western blot analysis with anti-NopM antibodies. Phosphorylation reactions with NtSIPK and NtMEK2^{DD} resulted in NopM forms that migrated more slowly on the gel. Similar results were also obtained for phosphorylation tests with NtSIPK combined with LjSIP2, a MAPK kinase from the legume *L. japonicus* (40). In contrast, reactions with NtMEK2^{DD} or LjSIP2 alone showed no effects on the apparent molecular weight of NopM, indicating that NopM was not phosphorylated by these MAPK kinases. These results showed that NopM was phosphorylated by NtSIPK (Fig. 6*D*).

To examine whether NopM was also phosphorylated in *L. japonicus*, we performed dephosphorylation experiments with extracts from C338A-expressing roots obtained by *A. rhizogenes*-mediated transformation. C338A was used for these tests because Western blot signals for C338A were much stronger than those for NopM. Aliquots of root extracts containing C338A were treated with or without APase. An additional protein sample contained Na_3VO_4, an APase inhibitor. The Western blotting results indicated that C338A was also phosphorylated in *L. japonicus* cells (Fig. 6*E*).

Discussion

Like IpaH family effectors of pathogenic bacteria, NopM of *Sinorhizobium* sp. NGR234 is thought to exploit the host ubiquitination pathway by functionally mimicking eukaryotic E3 ubiquitin ligases of the host cell. Accordingly, NopM, but not the enzymatically inactive variant C338A, promoted nodule formation in *L. purpureus*, indicating a positive effect on symbiosis (11, 17). Here, we report that NopM can have negative effects when directly expressed in plant cells. NopM, but not

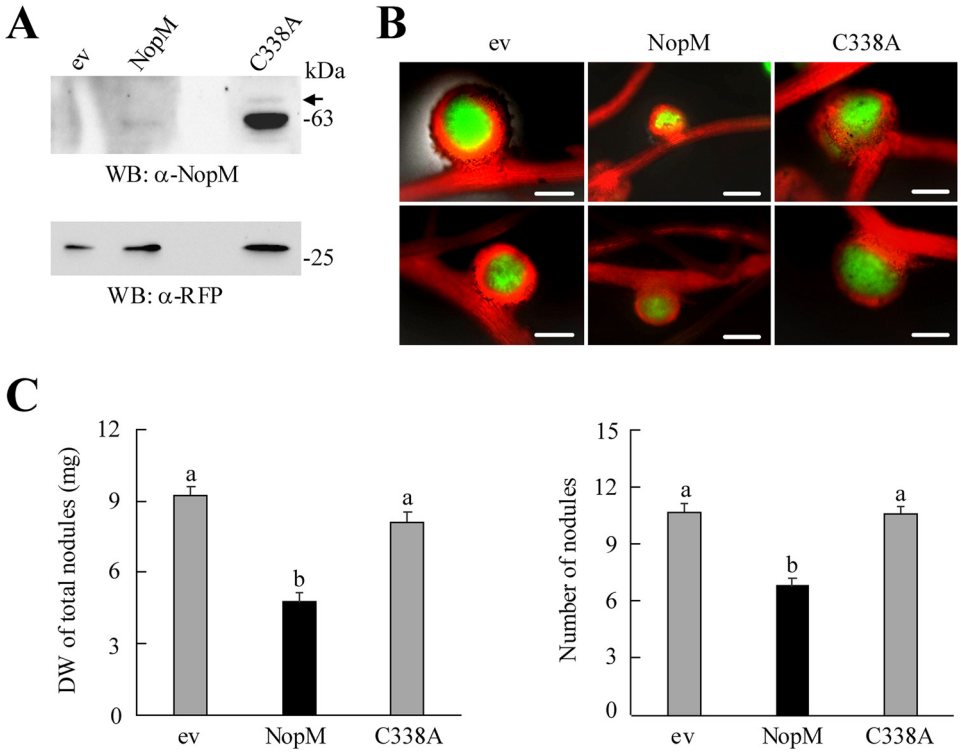

Figure 5. Expression of NopM and C338A in *L. japonicus* roots. *Agrobacterium rhizogenes*-mediated transformation was used to obtain transgenic roots expressing NopM or the enzymatically inactive variant C338A. Plants transformed with the empty vector (*ev*) containing an RFP expression cassette were used as a negative control. *A,* proteins from transgenic roots were isolated 30 days after transformation, and 5 μl of extracts were used for Western blot (*WB*) analysis with anti-NopM and anti-RFP antibodies. *B,* examples of pink nodules formed on the transformed *L. japonicus* roots 25 days after inoculation with *M. loti* MAFF303099 (GFP). Transgenic roots show RFP expression (*red fluorescence*). Green fluorescence indicates the presence of bacteria within nodules. *Bars,* 500 μm. *C,* quantification of nodule biomass (dry weight (*DW*)) and number of formed nodules per plant. Data indicate mean ± S.E. ($n = 10$). NopM-expressing roots formed significantly fewer nodules (*different letters* indicate differences; Kruskal-Wallis test, $p < 0.05$).

the enzymatically inactive variant C338A, induced cell death in tobacco, providing evidence that ubiquitination events culminated in effector-triggered immunity (Fig. 4). The NEL form could also induce cell death, but the response was overall less strong as for full-length NopM, suggesting that the presence of an LRR domain increased the NopM effector activity in this plant. This is reminiscent of the E3 ubiquitin ligase effector XopL of *Xanthomonas campestris*, which induces cell death in *N. benthamiana* (41). We suggest that NopM expressed in tobacco leaves ubiquitinates a host protein, which is guarded by a plant resistance protein. The cell death–inducing characteristics of NopM are reminiscent of the rhizobial T3 effector NopT, a protease inducing rapid cell death in tobacco and *A. thaliana* (42, 43). When expressed in the legume *L. japonicus*, NopM negatively affected nodulation with *M. loti*, suggesting an ETI-like response (15). Expression of the C338A variant did not influence nodulation, indicating that the observed asymbiotic role of NopM in *L. japonicus* cells depends on its E3 ubiquitin ligase activity (Fig. 5). Hence, ubiquitination of host proteins appears to promote (*L. purpureus*) or to reduce (*L. japonicus*) nodulation depending on the examined legume species. Such opposite effects on nodulation were also observed for other rhizobial T3 effectors. NopT of strain NGR234, for example, influenced nodule formation either positively or negatively depending on the host plant (17, 42).

When expressed in tobacco, NopM was phosphorylated at serine 26, a residue in the N-terminal region of the protein. Further *in vitro* phosphorylation tests showed that NopM was phosphorylated by NtSIPK (Fig. 6). To our knowledge, phosphorylation of a NEL domain E3 ubiquitin ligase has not been reported so far, but AvrPtoB, an E3 ubiquitin ligase effector of *Pseudomonas syringae*, was found to be phosphorylated by the tomato protein kinase Pto. Phosphorylation inhibits the E3 ubiquitin ligase activity of AvrPtoB (44). Phosphorylated NopM, however, appears to possess enzyme activity because the S26A variant induced cell death in tobacco (Fig. 6*C*), a response that was not observed for enzymatically inactive C338A protein (Fig. 4*A*). The role of NopM phosphorylation in the nodule symbiosis and host immune responses remains to be determined. Host MAPKs are good candidates to interact with NopM *in planta*, as NopM was found to be phosphorylated by NtSIPK *in vitro*. In this context it is worth noting that NopM could not ubiquitinate NtSIPK in our *in vitro* ubiquitination system (data not shown). Future experiments are required to examine whether MAPKs activate NopM function in plant cells or whether phosphorylated NopM is less active. It is worth mentioning that NopM interferes with mating pheromone signaling, suggesting that NopM has the capacity to impair MAPK signaling in yeast (11). Interactions with host MAPKs are perhaps required to impair activation of defense reactions that negatively influence nodule formation. However, our previous work showed that NopM expressed in *N. benthamiana* did not suppress expression of genes induced by MAPK signaling but inhibited formation of elicitor-induced ROS generation (11).

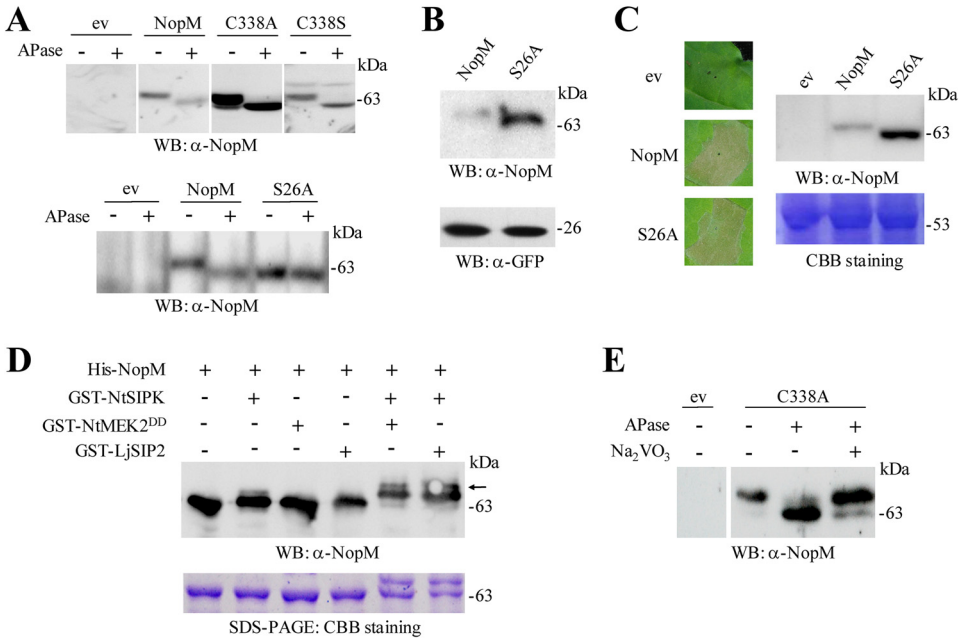

Figure 6. Phosphorylation of NopM *in planta* and *in vitro*. *A,* analysis of NopM and indicated variants isolated from tobacco leaves transformed with *A. tumefaciens*. Agrobacteria carrying the empty vector (*ev*) were used as negative control. Soluble proteins were extracted from the transformed leaf tissue, and aliquots were treated with APase. Samples were then subjected to Western blot (*WB*) analysis with anti-NopM antibodies. *B,* Western blot analysis of NopM and the S26A variant expressed in tobacco leaves. For comparison, co-expressed GFP was also analyzed in the obtained protein extracts. *C,* expression of the S26A variant in tobacco induces cell death. NopM expression and empty vector controls were used for comparison. The pictures were taken 3 days after infiltration with agrobacteria. A corresponding Western blot confirmed expression of the proteins. Coomassie Brilliant Blue (*CBB*) staining of ribulose-bisphosphate carboxylase/oxygenase large subunit in a parallel gel indicated the use of equal amounts of proteins. *D, in vitro* phosphorylation of NopM by NtSIPK. Indicated proteins with GST or His tags were expressed in *E. coli* and purified by affinity chromatography. The MAPK kinases NtMEK2^{DD} and LjSIP2 were used for activation of NtSIPK. Proteins were incubated in phosphorylation buffer containing ATP for 30 min at 30 °C. The samples were analyzed by Western blotting using an anti-NopM antibody. NopM phosphorylated by activated NtSIPK migrated more slowly on the gel (*upper bands marked by an arrow*). A parallel protein gel was stained with Coomassie Brilliant Blue. *E,* analysis of the C338A variant expressed in *L. japonicus* roots. Soluble proteins were extracted 28 days after transformation, and aliquots were treated with APase and 10 mM Na_3VO_4. Samples were then subjected to Western blot analysis with anti-NopM antibodies.

An interference with MAPK signaling has been recently shown for NopL, another T3 effector of NGR234. NopL possesses many phosphorylation sites and impairs MAPK signaling in a phosphorylation-dependent manner. NopL suppresses activation of plant defense responses and delays the senescence of nodules formed on *Phaseolus vulgaris* roots (8, 10, 12).

The subcellular distribution of NopM in different plant cell compartments suggests that potential target proteins of NopM are cytoplasmic proteins, membrane proteins, or nuclear proteins. Different members of the IpaH effector family exhibit various subcellular localization patterns, and the host cell itself may control effector targeting to specific subcellular compartments. For example, SspH2 of *S. enterica* is located at the plasma membranes of human cells due to *S*-palmitoylation (24, 45). Other effectors such as SspH1 of *S. enterica* and IpaH9.8 of *S. flexneri* are able to enter host nuclei (46, 47). The fluorescence signals produced in our BiFC experiments indicated a NopM–NopM interaction at plasma membranes. Dimerization of IpaH9.8 has been proposed to be important for its ability to form polyubiquitin chains *in vitro* (28). It remains to be examined whether phosphorylation of NopM by plant protein kinases precedes NopM–NopM complex formation and whether dimerization of NopM influences effector activity in plant cells.

IpaH family effectors such as SspH2 of *S. enterica* are autoregulated, *i.e.* the LRR domain inhibits the catalytic transfer of ubiquitin from the NEL domain to the substrate. A conformational change, presumably by binding of a given substrate to the LRR domain, activates the enzyme. Accordingly, proteins only consisting of the NEL domain show increased E3 ubiquitin ligase activity as compared with full-length proteins (20, 21, 24, 27, 48, 49). In accordance with such an autoinhibition mechanism, the enzyme activity of NopM was lower than that of a protein containing the NEL domain alone in our *in vitro* ubiquitination system (Fig. 1*A*). The performed enzyme tests also indicated that both NopM and the NEL alone preferentially form Lys-48–dependent unanchored polyubiquitin chains. Ubiquitination reactions with the K48R ubiquitin variant showed only weak activity to form unanchored polyubiquitin chains (Fig. 1, *B* and *C*). These results suggest that NopM, like other IpaH family effectors (22, 30), ubiquitinates host proteins to target them for proteasome-dependent proteolysis. In the absence of such substrates, NopM not only forms free polyubiquitin chains but also ubiquitinates itself. We observed that GST–NopM could ubiquitinate the enzymatically inactive variant C338A (Fig. 3*A*). Such auto-ubiquitination by an intermolecular transfer of ubiquitin is in agreement with the notion that LRR domains of IpaH family effectors are required for substrate binding. Many E3 ubiquitin ligases have the capacity to self-regulate their protein levels by ubiquitination and subsequent proteasome-dependent degradation (50). When expressed in plant cells, levels of NopM were lower than those of enzymatically inactive C338A, suggesting that NopM controls its own protein level through auto-ubiquitination.

Surprisingly, auto-ubiquitination was not abolished when all three lysine residues in NopM were substituted by arginine (His-tagged K3xR variant; Fig. 2). Hence, the protein was apparently ubiquitinated at one or several nonlysine residues. In *A. thaliana* for example, lysine residues in IAA1 (indole-3-acetic acid 1) were not required for proteasome-mediated degradation (51). Noncanonical ubiquitination of proteins by various E3 ubiquitin ligases was reported for threonine and serine residues (oxyester bonds), for cysteine residues (thioester bond), and for N-terminal amino acid residues (peptide bonds) (35, 36). Proteolytic removal of the N-terminal His tag resulted in a band shift of ubiquitinated K3xR forms, indicating that the protein remained, at least in part, ubiquitinated (Fig. 2*B*). Furthermore, His–K3xR with a C338A substitution could be ubiquitinated by GST–NopM (Fig. 2*D*). This substrate does not possess any cysteine residues, indicating that ubiquitin was not linked via a thioester bond. We therefore hypothesize that auto-ubiquitination of K3xR requires oxyester bond formation. Unfortunately, MS analysis of trypsin-digested mono-ubiquitinated His–K3xR–C338A failed to provide conclusive data (not shown), and future work will be required to identify ubiquitin attachment sites in K3xR.

In conclusion, this study provides evidence that NopM can be post-translationally modified in two ways, namely by phosphorylation and conjugation to ubiquitin. Whether phosphorylation influences MAPK signaling, auto-ubiquitination, or proteasome-dependent proteolysis of target proteins in plants remains to be studied. Our observation that GST–NopM could apparently ubiquitinate His–K3xR–C338A raises the exciting possibility that NopM can ubiquitinate plant proteins without lysine residues. We are currently making efforts to identify NopM substrates in plant cells.

Experimental procedures

Strains, plasmids, NopM variants, and primers

Details on bacterial strains and plasmids used in this study can be found in Table S1. NopM and protein variants of *Sinorhizobium* sp. NGR234 (C338A, C338S, S26A, K3xR, K3xR–C338A, NEL, and NEL–C338A) are shown in Figs. S1 and S2. The primers used are listed in Table S2.

Expression of proteins in E. coli

The protein expression vectors pET28a (with a His tag) or pGEX-4T-1 (with a GST tag) were used to obtain recombinant proteins from *E. coli*. The following proteins were expressed: E1 (At5g06460) of *A. thaliana*; E2 (At5g53300) of *A. thaliana*; ubiquitin (At4g02890) of *A. thaliana* and ubiquitin variants (lysine to arginine substitutions K6R, K11R, K27R, K29R, K33R, K48R, and K63R) (52, 53); UbΔGG (*A. thaliana* Ub lacking C-terminal di-glycine residues) (54); NopM of *Sinorhizobium* sp. NGR234 (NP_443862) and variants (Fig. S2); NtSIPK of tobacco (*Nicotiana tabacum*; U94192); the constitutively active MAPK kinase NtMEK2^{DD} of tobacco (AF325168) (38, 39); the MAPK kinase LjSIP2 of *L. japonicus* (HQ910409) (40); and USP5 of *Homo sapiens* (AAH05139.1) (33). Furthermore, DNA encoding Flag-tagged NopM and variants (C338A and C338S) was cloned into pET28a. *E. coli* BL21 (DE3) cells carrying a given plasmid were incubated at 18 °C for 24 h in the presence of 0.75 mM isopropyl β-D-thiogalactopyranoside to induce the expression of recombinant proteins. Cell pellets were collected for further protein purification using nickel-nitrilotriacetic acid beads (Qiagen, Hilden, Germany) and GSH-agarose beads (Novagen, Madison, WI), respectively. Quantities of purified proteins were determined by the Bradford method using commercially available BSA as a reference (55).

SDS-PAGE and Western blot analysis

Protein samples were analyzed by SDS-PAGE. Proteins were visualized by Coomassie Brilliant Blue staining. For Western blot analysis, proteins were transferred to nitrocellulose membranes. When appropriate, membranes were stained with Ponceau S. Membranes were probed with specific antibodies, namely against NopM (11), GFP (TransGen Biotech, Beijing, China), RFP (TransGen Biotech, Beijing, China), ubiquitin (Santa Cruz Biotechnology, Dallas, TX), GST (TransGen Biotech, Beijing, China), or the Flag epitope (TransGen Biotech, Beijing, China). Immunoblots were developed with 3,3′-diaminobenzidine from Boster (Wuhan, China) or enhanced chemiluminescence reagents from GE Healthcare.

In vitro ubiquitination assay

Ubiquitination reactions (30-μl test volume) were carried out in 25 mM Tris-HCl (pH 7.5) buffer supplemented with 50 mM NaCl, 5 mM ATP, 10 mM $MgCl_2$, 0.1 mM DTT, 2 μg of ubiquitin (His-ubiquitin or variants; GST-ubiquitin), 0.5 μg of His-AtUBA2 (E1), and 1 μg of His-AtUBC10 (E2) in the presence or absence of 2 μg of His–NopM or variants (E3). Where indicated, human USP5 cleaving unanchored polyubiquitin chains (33) was added to the reaction. For analysis of intermolecular transfer of His-tagged ubiquitin from active NopM to inactive NopM variants (Figs. 2*D* and 3*A*), the ubiquitination reactions contained 1 μg of active NopM and 2 μg of an inactive NopM variant. Samples of ubiquitination reactions were incubated at 37 °C for 1.5 h if not otherwise specified. Finally, reaction mixtures were subjected to SDS-PAGE and Western blot analysis with anti-ubiquitin, anti-NopM, anti-Flag, or anti-GST antibodies.

Where indicated, ubiquitinated His–K3xR (NopM variant in which the three lysines were substituted by arginine) without the N-terminal His tag was analyzed. Equal amounts of His–K3xR and commercial ubiquitin without His tag (Boston-Biochem) were used in the ubiquitination reaction system. After incubation, reactions were quenched by adding 8 IU of apyrase (28), and the sample was incubated with 4 IU of thrombin (Sigma) at 16 °C for 6 h.

BiFC and subcellular localization analyses

NopM–NopM interactions in epidermal onion (*Alium cepa*) cells were analyzed by a BiFC approach. The vector pSAT1–nEYFP–N1 contained the N-terminal coding sequence of enhanced yellow fluorescent protein (nYFP) and pSAT1-cEYFP-N1 contained the corresponding C-terminal coding sequence (cYFP). The sequence encoding NopM was inserted into these vectors to produce recombinant NopM–nYFP and NopM–cYFP (Table S1). BiFC analysis of onion cells transformed by particle bombardment (PDS-1000/He particle deliv-

ery system, Bio-Rad) was performed as reported previously (12). Cells were analyzed by a TCS SP2 laser confocal microscope (Leica, Wetzlar, Germany), and the excitation wavelength of the laser beam was adjusted to 514 nm for detection of yellow fluorescence.

For subcellular localization analysis in onion cells, the sequence encoding NopM was inserted into pX-DR and pCAMBIA-1302 (Table S1). The resulting plasmids encoding NopM fused to fluorescent proteins (RFP and GFP) were transformed into epidermal cells by microprojectile bombardment as for the BiFC experiments. Furthermore, subcellular localization analysis of NopM or C338A fused to GFP (pCAMBIA-1302 constructs) was studied in *A. thaliana* ecotype Columbia (Col-0) protoplasts. Preparation of protoplasts and transformation with the help of PEG 4000 were performed as described (56). The nuclear marker ARF4 (auxin response factor 4; AED97332.1) fused to RFP was co-transformed. Transformed onion and *A. thaliana* protoplasts were analyzed by confocal microscopy. The excitation wavelength of the laser beam was adjusted to 561 nm (red fluorescence) and 488 nm (green fluorescence), respectively.

Expression of NopM and variants in plants and preparation of protein extracts

For tobacco (*N. tabacum* cv. Xanthi) leaf transformation, *A. tumefaciens* EHA105 carrying pCAMBIA1302 containing a GFP expression cassette was used. The constructs (expression of NopM and the variants C338A, C338S, NEL, and S26A; Fig. S2) contained a CaMV 35S promoter. Agrobacteria were infiltrated into tobacco leaves as described (10) with some modifications. EHA105 strains were grown overnight at 27 °C in LB medium. Cell pellets were collected and resuspended in 10 mM $MgSO_4$ supplemented with 200 μM acetosyringone to reach A_{600} (absorbance at 600 nm) ≈0.6. Soluble proteins were extracted from leaves 2 days post-infiltration, as reported previously (8), using 1 ml of extraction buffer per g of leaf (fresh weight). Photographs of infiltrated leaves were taken 3 days post-infiltration with agrobacteria. In addition, leaves were boiled for 5 min in ethanol to improve visualization of necrotic cells.

A. rhizogenes LBA9402 was used for generation of transgenic *L. japonicus* (ecotype MG20) roots expressing NopM or the enzymatically inactive variant C338A. Transformation was performed according to a previously described procedure (57). The binary vector pISV(RFP) contained an RFP expression cassette to visualize the transformed tissue. The transgenic roots expressed constructs encoding NopM or C338A under the control of a tandem CaMV 35S promoter. For transformation, agrobacteria carrying corresponding plasmids were grown on YMB (0.4 g liter^{-1} yeast extract, 2 g liter^{-1} mannitol, and 0.1 g liter^{-1} NaCl (pH 7.0)) agar plates at 27 °C for 4–5 days. Hypocotyls of *L. japonicus* seedlings (5–7 days old), germinated on 0.8% (w/v) water agar plates, were cut, and the remaining upper parts of seedlings were dipped into LBA9402 bacteria on the YMB agar plates for 15 min. Plants were then transferred to 0.8% (w/v) water agar slants containing Gamborg's 1/2 B5 salts and vitamin media (58). The plates were placed nearly vertically at 22 °C in a growth room (8 h dark and 16 h light). Every 7–10 days, seedlings were transferred to freshly-made plates. Roots at 30 days after transformation were examined by fluorescence microscopy (RFP detection), and transgenic roots were used for protein extraction and Western blot analysis as described above for tobacco plants.

Nodulation tests

L. japonicus roots co-expressing RFP and NopM or the C338A variant were used for inoculation tests. RFP-expressing roots transformed with the empty vector pISV(RFP) served as a control. At 30 days post-transformation, nontransgenic roots (lacking RFP expression) were removed, and 10 plants of each construct were placed into Magenta jars (1 plant per jar) containing vermiculite in the upper jar and nutrient solution containing 0.5 mM KNO_3 in the lower jar. One week later, the plants were inoculated with the GFP-expressing strain *M. loti* MAFF303099 (GFP). Nodules were harvested 25 days later and analyzed by fluorescence microscopy. The biomass (dry weight) of nodules and the number of nodules were quantified for each plant. Statistical analysis was performed with the Kruskal-Wallis rank sum test, and a p value of ≤0.05 was considered as significant.

Phosphorylation and dephosphorylation assays

In vitro phosphorylation experiments were performed to test whether NopM is a MAPK substrate. A typical reaction mixture (30 μl) contained GST-tagged NtSIPK (0.25 μg μl^{-1}), GST-tagged NtMEK2^{DD} (0.25 μg μl^{-1}), or GST-tagged LjSIP2 (0.25 μg μl^{-1}) and His-tagged NopM (0.75 μg μl^{-1}), 20 mM HEPES-KOH (pH 7.6), 1 mM DTT, 10 mM $MgCl_2$, and 50 μM ATP (12). Samples were incubated at 30 °C for 30 min and directly used for SDS-PAGE and Western blot analysis with anti-NopM antibodies.

To analyze NopM phosphorylation *in vivo*, soluble proteins of tobacco plants expressing NopM and variants (C338A, C338S, or S26A) were incubated with APase. Proteins from *L. japonicus* expressing NopM and the C338A variant were examined in a similar way. A typical dephosphorylation reaction contained the protein extract (25 μl) and 4 units of calf intestine APase (ThermoFisher Scientific, Waltham, MA). Samples were incubated at 37 °C for 1 h, and dephosphorylation of NopM and variants (band shift) was analyzed on Western blots with anti-NopM antibodies.

Author contributions—C.-C. X. designed the experiments, analyzed the corresponding results, and wrote the paper; D. Z. designed the experiments and analyzed the corresponding results; D. R. H. wrote the paper; Z.-P. X. and C. S. designed the experiments, analyzed the corresponding results, and wrote the paper.

Acknowledgments—We thank Dr. Ying-Ying Ge and Dr. Qi-Qiang Xiang for help with phosphorylation and BiFC experiments. Feng Yang and Peng-Fei Zhu are acknowledged for construction of pISV(RFP), pISV(RFP)-nopM, and pISV(RFP)-nopM(C338A). We are grateful to Prof. Jian-Feng Li (Sun Yat-sen University, Guangzhou, China) for advice with A. thaliana protoplast transformations.

References

1. Galán, J. E., Lara-Tejero, M., Marlovits, T. C., and Wagner, S. (2014) Bacterial type III secretion systems: specialized nanomachines for protein delivery into target cells. *Annu. Rev. Microbiol.* **68,** 415–438 CrossRef Medline
2. Marín, M., Uversky, V. N., and Ott, T. (2013) Intrinsic disorder in pathogen effectors: protein flexibility as an evolutionary hallmark in a molecular arms race. *Plant Cell* **25,** 3153–3157 CrossRef Medline
3. Büttner, D. (2016) Behind the lines–actions of bacterial type III effector proteins in plant cells. *FEMS Microbiol. Rev.* **40,** 894–937 CrossRef Medline
4. Cui, H., Tsuda, K., and Parker, J. E. (2015) Effector-triggered immunity: from pathogen perception to robust defense. *Annu. Rev. Plant Biol.* **66,** 487–511 CrossRef Medline
5. Staehelin, C., and Krishnan, H. B. (2015) Nodulation outer proteins: double-edged swords of symbiotic rhizobia. *Biochem. J.* **470,** 263–274 CrossRef Medline
6. Nelson, M. S., and Sadowsky, M. J. (2015) Secretion systems and signal exchange between nitrogen-fixing rhizobia and legumes. *Front. Plant Sci.* **6,** 491 Medline
7. Perret, X., Staehelin, C., and Broughton, W. J. (2000) Molecular basis of symbiotic promiscuity. *Microbiol. Mol. Biol. Rev.* **64,** 180–201 CrossRef Medline
8. Bartsev, A. V., Deakin, W. J., Boukli, N. M., McAlvin, C. B., Stacey, G., Malnoë, P., Broughton, W. J., and Staehelin, C. (2004) NopL, an effector protein of *Rhizobium* sp. NGR234, thwarts activation of plant defense reactions. *Plant Physiol.* **134,** 871–879 CrossRef Medline
9. López-Baena, F. J., Monreal, J. A., Pérez-Montaño, F., Guasch-Vidal, B., Bellogín, R. A., Vinardell, J. M., and Ollero, F. J. (2009) The absence of Nops secretion in *Sinorhizobium fredii* HH103 increases GmPR1 expression in Williams soybean. *Mol. Plant Microbe Interact.* **22,** 1445–1454 CrossRef Medline
10. Zhang, L., Chen, X. J., Lu, H. B., Xie, Z. P., and Staehelin, C. (2011) Functional analysis of the type 3 effector nodulation outer protein L (NopL) from *Rhizobium* sp. NGR234: symbiotic effects, phosphorylation, and interference with mitogen-activated protein kinase signaling. *J. Biol. Chem.* **286,** 32178–32187 CrossRef Medline
11. Xin, D. W., Liao, S., Xie, Z. P., Hann, D. R., Steinle, L., Boller, T., and Staehelin, C. (2012) Functional analysis of NopM, a novel E3 ubiquitin ligase (NEL) domain effector of *Rhizobium* sp. strain NGR234. *PLoS Pathog.* **8,** e1002707 CrossRef Medline
12. Ge, Y. Y., Xiang, Q. W., Wagner, C., Zhang, D., Xie, Z. P., and Staehelin, C. (2016) The type 3 effector NopL of *Sinorhizobium* sp. strain NGR234 is a mitogen-activated protein kinase substrate. *J. Exp. Bot.* **67,** 2483–2494 CrossRef Medline
13. Okazaki, S., Kaneko, T., Sato, S., and Saeki, K. (2013) Hijacking of leguminous nodulation signaling by the rhizobial type III secretion system. *Proc. Natl. Acad. Sci. U.S.A.* **110,** 17131–17136 CrossRef Medline
14. Yang, S., Tang, F., Gao, M., Krishnan, H. B., and Zhu, H. (2010) R gene-controlled host specificity in the legume–rhizobia symbiosis. *Proc. Natl. Acad. Sci. U.S.A.* **107,** 18735–18740 CrossRef Medline
15. Yasuda, M., Miwa, H., Masuda, S., Takebayashi, Y., Sakakibara, H., and Okazaki, S. (2016) Effector-triggered immunity determines host genotype-specific incompatibility in legume–*Rhizobium* symbiosis. *Plant Cell Physiol.* **57,** 1791–1800 CrossRef Medline
16. Rodrigues, J. A., López-Baena, F. J., Ollero, F. J., Vinardell, J. M., Espuny Mdel, R., Bellogín, R. A., Ruiz-Sainz, J. E., Thomas, J. R., Sumpton, D., Ault, J., and Thomas-Oates, J. (2007) NopM and NopD are rhizobial nodulation outer proteins: identification using LC-MALDI and LC-ESI with a monolithic capillary column. *J. Proteome Res.* **6,** 1029–1037 CrossRef Medline
17. Kambara, K., Ardissone, S., Kobayashi, H., Saad, M. M., Schumpp, O., Broughton, W. J., and Deakin, W. J. (2009) Rhizobia utilize pathogen-like effector proteins during symbiosis. *Mol. Microbiol.* **71,** 92–106 CrossRef Medline
18. Chen, M., Xiang, Q. W., Ge, Y. Y., Huang, Q. Y., Liang, Y., Xu, C. C., Zhang, D., Zhang, M. X., Zhu, P. F., Xie, Z. P., and Staehelin, C. (2016) Use of a *Xanthomonas*/pepper translocation system for characterization of rhizobial type 3 effectors. In *Recent Trends in PGPR Research for Sustainable Crop Productivity* (Sayyed, R. Z., Reddy, M. S., and Al-Turki, A. I., eds) pp. 174–178, Scientific Publishers, Jodhpurt, India
19. Rohde, J. R., Breitkreutz, A., Chenal, A., Sansonetti, P. J., and Parsot, C. (2007) Type III secretion effectors of the IpaH family are E3 ubiquitin ligases. *Cell Host Microbe* **1,** 77–83 CrossRef Medline
20. Singer, A. U., Rohde, J. R., Lam, R., Skarina, T., Kagan, O., Dileo, R., Chirgadze, N. Y., Cuff, M. E., Joachimiak, A., Tyers, M., Sansonetti, P. J., Parsot, C., and Savchenko, A. (2008) Structure of the *Shigella* T3SS effector IpaH defines a new class of E3 ubiquitin ligases. *Nat. Struct. Mol. Biol.* **15,** 1293–1301 CrossRef Medline
21. Zhu, Y., Li, H., Hu, L., Wang, J., Zhou, Y., Pang, Z., Liu, L., and Shao, F. (2008) Structure of a *Shigella* effector reveals a new class of ubiquitin ligases. *Nat. Struct. Mol. Biol.* **15,** 1302–1308 CrossRef Medline
22. Ashida, H., and Sasakawa, C. (2015) *Shigella* IpaH family effectors as a versatile model for studying pathogenic bacteria. *Front. Cell. Infect. Microbiol.* **5,** 100 Medline
23. Bernal-Bayard, J., and Ramos-Morales, F. (2009) *Salmonella* type III secretion effector SlrP is an E3 ubiquitin ligase for mammalian thioredoxin. *J. Biol. Chem.* **284,** 27587–27595 CrossRef Medline
24. Quezada, C. M., Hicks, S. W., Galán, J. E., and Stebbins, C. E. (2009) A family of *Salmonella* virulence factors functions as a distinct class of autoregulated E3 ubiquitin ligases. *Proc. Natl. Acad. Sci. U.S.A.* **106,** 4864–4869 CrossRef Medline
25. Nakano, M., Oda, K., and Mukaihara, T. (2017) *Ralstonia solanacearum* novel E3 ubiquitin ligase (NEL) effectors RipAW and RipAR suppress pattern-triggered immunity in plants. *Microbiology* **163,** 992–1002 CrossRef Medline
26. Zheng, N., and Shabek, N. (2017) Ubiquitin ligases: structure, function, and regulation. *Annu. Rev. Biochem.* **86,** 129–157 CrossRef Medline
27. Keszei, A. F., and Sicheri, F. (2017) Mechanism of catalysis, E2 recognition, and autoinhibition for the IpaH family of bacterial E3 ubiquitin ligases. *Proc. Natl. Acad. Sci. U.S.A.* **114,** 1311–1316 CrossRef Medline
28. Edwards, D. J., Streich, F. C., Jr., Ronchi, V. P., Todaro, D. R., and Haas, A. L. (2014) Convergent evolution in the assembly of polyubiquitin degradation signals by the *Shigella flexneri* IpaH9.8 ligase. *J. Biol. Chem.* **289,** 34114–34128 CrossRef Medline
29. Li, P., Jiang, W., Yu, Q., Liu, W., Zhou, P., Li, J., Xu, J., Xu, B., Wang, F., and Shao, F. (2017) Ubiquitination and degradation of GBPs by a *Shigella* effector to suppress host defence. *Nature* **551,** 378–383 Medline
30. Wandel, M. P., Pathe, C., Werner, E. I., Ellison, C. J., Boyle, K. B., von der Malsburg, A., Rohde, J., and Randow, F. (2017) GBPs inhibit motility of *Shigella flexneri* but are targeted for degradation by the bacterial ubiquitin ligase IpaH9.8. *Cell Host Microbe* **22,** 507–518.e5 CrossRef Medline
31. Seyedarabi, A., Sullivan, J. A., Sasakawa, C., and Pickersgill, R. W. (2010) A disulfide driven domain swap switches off the activity of *Shigella* IpaH9.8 E3 ligase. *FEBS Lett.* **584,** 4163–4168 CrossRef Medline
32. Valkevich, E. M., Sanchez, N. A., Ge, Y., and Strieter, E. R. (2014) Middle-down mass spectrometry enables characterization of branched ubiquitin chains. *Biochemistry* **53,** 4979–4989 CrossRef Medline
33. Wilkinson, K. D., Tashayev, V. L., O'Connor, L. B., Larsen, C. N., Kasperek, E., and Pickart, C. M. (1995) Metabolism of the polyubiquitin degradation signal: structure, mechanism, and role of isopeptidase T. *Biochemistry* **34,** 14535–14546 CrossRef Medline
34. Breitschopf, K., Bengal, E., Ziv, T., Admon, A., and Ciechanover, A. (1998) A novel site for ubiquitination: the N-terminal residue, and not internal lysines of MyoD, is essential for conjugation and degradation of the protein. *EMBO J.* **17,** 5964–5973 CrossRef Medline
35. McDowell, G. S., and Philpott, A. (2013) Non-canonical ubiquitylation: mechanisms and consequences. *Int. J. Biochem. Cell Biol.* **45,** 1833–1842 CrossRef Medline
36. Wang, X., Herr, R. A., and Hansen, T. H. (2012) Ubiquitination of substrates by esterification. *Traffic* **13,** 19–24 CrossRef Medline
37. Pearson, R. B., and Kemp, B. E. (1991) Protein kinase phosphorylation site sequences and consensus specificity motifs: tabulations. *Methods Enzymol.* **200,** 62–81 CrossRef Medline

38. Yang, K. Y., Liu, Y., and Zhang, S. (2001) Activation of a mitogen-activated protein kinase pathway is involved in disease resistance in tobacco. *Proc. Natl. Acad. Sci. U. S. A.* **98,** 741–746 CrossRef Medline
39. Zhang, S., and Liu, Y. (2001) Activation of salicylic acid–induced protein kinase, a mitogen-activated protein kinase, induces multiple defense responses in tobacco. *Plant Cell* **13,** 1877–1889 CrossRef Medline
40. Chen, T., Zhu, H., Ke, D., Cai, K., Wang, C., Gou, H., Hong, Z., and Zhang, Z. (2012) A MAP kinase kinase interacts with SymRK and regulates nodule organogenesis in *Lotus japonicus*. *Plant Cell* **24,** 823–838 CrossRef Medline
41. Singer, A. U., Schulze, S., Skarina, T., Xu, X., Cui, H., Eschen-Lippold, L., Egler, M., Srikumar, T., Raught, B., Lee, J., Scheel, D., Savchenko, A., and Bonas, U. (2013) A pathogen type III effector with a novel E3 ubiquitin ligase architecture. *PLoS Pathog.* **9,** e1003121 CrossRef Medline
42. Dai, W. J., Zeng, Y., Xie, Z. P., and Staehelin, C. (2008) Symbiosis-promoting and deleterious effects of NopT, a novel type 3 effector of *Rhizobium* sp. strain NGR234. *J. Bacteriol.* **190,** 5101–5110 CrossRef Medline
43. Fotiadis, C. T., Dimou, M., Georgakopoulos, D. G., Katinakis, P., and Tampakaki, A. P. (2012) Functional characterization of NopT1 and NopT2, two type III effectors of *Bradyrhizobium japonicum*. *FEMS Microbiol. Lett.* **327,** 66–77 CrossRef Medline
44. Ntoukakis, V., Mucyn, T. S., Gimenez-Ibanez, S., Chapman, H. C., Gutierrez, J. R., Balmuth, A. L., Jones, A. M., and Rathjen, J. P. (2009) Host inhibition of a bacterial virulence effector triggers immunity to infection. *Science* **324,** 784–787 CrossRef Medline
45. Hicks, S. W., Charron, G., Hang, H. C., and Galán, J. E. (2011) Subcellular targeting of *Salmonella* virulence proteins by host-mediated *S*-palmitoylation. *Cell Host Microbe* **10,** 9–20 CrossRef Medline
46. Toyotome, T., Suzuki, T., Kuwae, A., Nonaka, T., Fukuda, H., Imajoh-Ohmi, S., Toyofuku, T., Hori, M., and Sasakawa, C. (2001) *Shigella* protein IpaH9.8 is secreted from bacteria within mammalian cells and transported to the nucleus. *J. Biol. Chem.* **276,** 32071–32079 CrossRef Medline
47. Haraga, A., and Miller, S. I. (2003) A *Salmonella enterica* serovar *typhimurium* translocated leucine-rich repeat effector protein inhibits NF-κB-dependent gene expression. *Infect. Immun.* **71,** 4052–4058 CrossRef Medline
48. Chou, Y. C., Keszei, A. F., Rohde, J. R., Tyers, M., and Sicheri, F. (2012) Conserved structural mechanisms for autoinhibition in IpaH ubiquitin ligases. *J. Biol. Chem.* **287,** 268–275 CrossRef Medline
49. Zouhir, S., Bernal-Bayard, J., Cordero-Alba, M., Cardenal-Muñoz, E., Guimaraes, B., Lazar, N., Ramos-Morales, F., and Nessler, S. (2014) The structure of the Slrp–Trx1 complex sheds light on the autoinhibition mechanism of the type III secretion system effectors of the NEL family. *Biochem. J.* **464,** 135–144 CrossRef Medline
50. de Bie, P., and Ciechanover, A. (2011) Ubiquitination of E3 ligases: self-regulation of the ubiquitin system via proteolytic and non-proteolytic mechanisms. *Cell Death Differ.* **18,** 1393–1402 CrossRef Medline
51. Gilkerson, J., Kelley, D. R., Tam, R., Estelle, M., and Callis, J. (2015) Lysine residues are not required for proteasome-mediated proteolysis of the auxin/indole acidic acid protein IAA1. *Plant Physiol.* **168,** 708–720 CrossRef Medline
52. Zhao, Q., Tian, M., Li, Q., Cui, F., Liu, L., Yin, B., and Xie, Q. (2013) A plant-specific *in vitro* ubiquitination analysis system. *Plant. J.* **74,** 524–533 CrossRef Medline
53. Komander, D., and Rape, M. (2012) The ubiquitin code. *Annu. Rev. Biochem.* **81,** 203–229 CrossRef Medline
54. Park, Y., Yoon, S. K., and Yoon, J. B. (2009) The HECT domain of TRIP12 ubiquitinates substrates of the ubiquitin fusion degradation pathway. *J. Biol. Chem.* **284,** 1540–1549 CrossRef Medline
55. Bradford, M. M. (1976) A rapid and sensitive method for the quantitation of microgram quantities of protein utilizing the principle of protein-dye binding. *Anal. Biochem.* **72,** 248–254 CrossRef Medline
56. Wu, F. H., Shen, S. C., Lee, L. Y., Lee, S. H., Chan, M. T., and Lin, C. S. (2009) Tape-*Arabidopsis* sandwich–a simpler *Arabidopsis* protoplast isolation method. *Plant Methods* **5,** 16 CrossRef Medline
57. Kumagai, H., and Kouchi, H. (2003) Gene silencing by expression of hairpin RNA in *Lotus japonicus* roots and root nodules. *Mol. Plant Microbe Interact.* **16,** 663–668 CrossRef Medline
58. Gamborg, O. L. (1970) The effects of amino acids and ammonium on the growth of plant cells in suspension culture. *Plant Physiol.* **45,** 372–375 CrossRef Medline